Title: Octupole correlations in the N = Z + 2 = 56 110Xe nucleus

Phys. Lett. B 848 (2024) 138371

Contents lists available at ScienceDirect

Physics Letters B

journal homepage: www.elsevier.com/locate/physletb

Letter

Octupole correlations in the N = Z + 2 = 56 ^{110}Xe nucleus

A. Illana [a,b,*], R.M. Pérez-Vidal [c,d,*], D. Stramaccioni [c,e], J.J. Valiente-Dobón [c], T.R. Rodriguez [f,b], L.M. Robledo [f], A. Poves [g], K. Auranen [a], O. Beliuskina [a], C. Delafosse [a,1], T. Eronen [a], Z. Ge [a,2], S. Geldhof [a,3], W. Gins [a], T. Grahn [a], P.T. Greenlees [a], H. Joukainen [a], R. Julin [a], H. Jutila [a], A. Kankainen [a], M. Leino [a], J. Louko [a], M. Luoma [a], D. Nesterenko [a], J. Ojala [a,4], J. Pakarinen [a], P. Rahkila [a], P. Ruotsalainen [a], M. Sandzelius [a], J. Sarén [a], J. Uusitalo [a], G.L. Zimba [a]

[a] Accelerator Laboratory, Department of Physics, University of Jyväskylä, P.O. Box 35, FI-40014, University of Jyväskylä Finland
[b] Departamento de Estructura de la Materia, Física Térmica y Electrónica and IPARCOS, Universidad Complutense de Madrid, E-28040 Madrid, Spain
[c] Istituto Nazionale di Fisica Nucleare, Laboratori Nazionali di Legnaro, Legnaro, I-35020, Italy
[d] Instituto de Física Corpuscular, CSIC-Universidad de Valencia, Valencia, E-46980, Spain
[e] Dipartimento di Fisica e Astronomia dell'Università degli Studi di Padova, Padova, I-35131, Italy
[f] Departamento de Física Teórica and CIAFF, Universidad Autónoma de Madrid, E-28049 Madrid, Spain
[g] Departamento de Física Teórica and IFT, Universidad Autónoma de Madrid, E-28049 Madrid, Spain

ARTICLE INFO

Editor: B. Blank

Keywords:
Octupole deformations
^{110}Xe
$N = Z = 56$ region
Fusion evaporation reactions

ABSTRACT

This letter reports on the first observation of an octupole band in the neutron-deficient ($N = Z + 2$) nucleus ^{110}Xe. The ^{110}Xe nuclei were produced via the ^{54}Fe(^{58}Ni,2n) fusion-evaporation reaction. The emitted γ rays were detected using the JUROGAM 3 γ-ray spectrometer, while the fusion-evaporation residues were separated with the MARA separator at the Accelerator Laboratory of the University of Jyväskylä, Finland. The experimental observation of the low-lying 3^- and 5^- states and inter-band E1 transitions between the ground-state band and the octupole band proves the importance of octupole correlations in this region. These new experimental data combined with theoretical calculations using the symmetry-conserving configuration-mixing method, based on a Gogny energy density functional, have been interpreted as an evidence of enhanced octupole correlations in neutron-deficient xenon isotopes.

1. Introduction

Shapes in nuclei have been extensively investigated during the history of nuclear physics, and the present understanding is that the shape is determined by the collective motion of the interacting nucleons. The main shapes, spherical, prolate, and oblate, arise from the quadrupole deformations, where the nucleus retains both axial and reflection symmetry. In the case of a quadrupole-deformed even-even nucleus, the low-lying positive-parity states typically form a rotational band, and are connected by collective E2 transitions. However, certain nuclei with a specific combination of proton and neutron number can develop octupole deformation. Octupole-deformed nuclei have a reflection asymmetric or "pear" shape in the intrinsic frame, either in a dynamic way (octupole vibrations) or having a static shape (permanent octupole deformation). These octupole correlations are generated microscopically by the interaction between orbitals with opposite parity near the Fermi surface, which differ by three units of angular momentum. Such correlations happen in well-defined areas of the Segrè chart, when the number of protons or neutrons is close to 34, 56, 88, and 134. In even-even nuclei, the presence of low-lying negative-parity states, which are connected to the yrast band via intense E1 and E3 transitions, is inter-

* Corresponding authors.
E-mail addresses: andres.illana@ucm.es (A. Illana), rosa.maria.perez.vidal@lnl.infn.it (R.M. Pérez-Vidal).
[1] Present address: Université Paris-Saclay, IJCLab, CNRS/IN2P3, F-91405 Orsay, France.
[2] Present address: GSI Helmholtzzentrum für Schwerionenforschung GmbH, D-64291 Darmstadt, Germany.
[3] Present address: GANIL, CEA/DSM-CNRS/IN2P3, Bd Henri Becquerel, BP 55027, F-14076 Caen Cedex 5, France.
[4] Present address: Department of Physics, Oliver Lodge Laboratory, University of Liverpool, P.O. Box 147, Liverpool L69 7ZE, UK.

https://doi.org/10.1016/j.physletb.2023.138371
Received 31 March 2023; Received in revised form 2 November 2023; Accepted 28 November 2023
Available online 4 December 2023

preted as evidence of octupole correlations. Comprehensive reviews can be found in Refs. [1,2].

Octupole correlations in nuclei near $N = Z$ are unique in the sense that they occur between nucleons when both protons and neutrons occupy the same orbitals. For $N \sim 56$ and $Z \sim 56$, these correlations will be enhanced at low and medium spin in light Te ($Z = 52$), I ($Z = 53$) and Xe ($Z = 54$) nuclei [3]. In this region of the nuclear chart, the Fermi surface for both neutrons and protons lies close to orbitals originating from the $d_{5/2}$ and $h_{11/2}$ subshells. Hence, octupole correlations emerge from the interactions of valence nucleons outside the ^{100}Sn core in these orbitals [1,4]. Close to $N = Z = 56$, a level structure characteristic of octupole correlations, consisting of negative-parity states and enhanced E1 transitions, has been observed in several cases including ^{112}Xe [5], ^{114}Xe [6–8] and ^{118}Ba [9]. The reduced transition probability $B(E3; 3^- \rightarrow 0^+)$ has only been measured for one nucleus in this region, ^{114}Xe [8]. The value of 70 W.u. for ^{114}Xe is one of the largest values that has been experimentally measured. Hence, the identification of octupole structures for more neutron-deficient nuclei is of utmost importance.

To tackle this question, we have studied octupole correlations in the very exotic $N = Z + 2$ ^{110}Xe, $N = 56$, isotope, via the first identification of an octupole band and the E1 transitions connecting its three lowest states to the ground-state band. In the previous experiment performed by Sandzelius et al. [10], it was possible to identify the ground-state band up to the (6^+) state. In that measurement, there was no indication of the γ rays de-exciting from the octupole band, although some γ rays were not placed in the level scheme due to the limited γ-γ statistics. The unexpectedly low-level energies for the g.s. band were suggested to be due to enhanced collectivity, possibly arising from isoscalar neutron-proton interactions becoming increasingly important close to the $N = Z$ line [10]. However, subsequent large-shell model calculations performed by Caurier et al. [11] predicted the same behaviour arising from isovector paring. The present letter reports for the first time the identification of the octupole band, as well as its connection with the yrast band, in the extremely neutron-deficient ($N = Z+2$) nucleus ^{110}Xe. In addition, state-of-the-art theoretical Energy Density Functional (EDF) calculations were performed to understand octupole correlations, and determine the strength of the electromagnetic E1 and E3 transitions connecting the positive-parity ground-state band with the octupole band in this exotic region.

2. Experimental setup

The ^{110}Xe nuclei were produced via a fusion-evaporation reaction using a ^{58}Ni beam impinging on a gold-backed ^{54}Fe target. The ^{58}Ni beam, with an energy of 255 MeV and intensity of ~3 pnA, was provided by the K130 cyclotron at the Accelerator Laboratory of the University of Jyväskylä (JYFL) during 14 days of beam time. The target consisted of a 0.75 mg/cm^2 foil of ^{54}Fe isotopically enriched to 99.9%, and backed with 1.0 mg/cm^2 of ^{197}Au. The gold backing was facing the beam to defuse the thermal heat generated by the beam, and to extend the life and performance of the ^{54}Fe layer. The experimental setup consisted of the JUROGAM 3 γ-ray spectrometer [12] at the target position coupled to the Mass Analysing Recoil Apparatus (MARA) vacuum mode-recoil separator [13,14]. In this configuration, prompt γ rays emitted at the target position were detected with an absolute efficiency of 4.5% at 1.3 MeV by the JUROGAM 3 array.

The fusion-evaporation residues, hereafter referred to as recoils, were separated from the beam-like and target-like products according to their mass-to-charge state ratio (A/q) by the MARA recoil separator. The ions are transported to the MARA focal plane through a Multi-Wire Proportional Counter (MWPC) and implanted into a BB20-type Double-sided Silicon Strip Detector (DSSD). This detector has 192 × 72 strips, each with a width of 0.67 mm, and a thickness of 300 μm [14]. The mass slits on both sides of the MWPC permit the selection of the A/q range around the region of interest, and almost suppress the unwanted masses that could overload the DSSD, hence, increasing the possibility to lose the recoil-decay correlations. The mass slits were set up to enhance the correlations of nuclei with mass number $A = 110$. Nuclei of interest were then identified by employing the Recoil-Decay Tagging (RDT) technique [15–17] and subsequently correlated with prompt γ rays emitted at the target position. All the signals were time-stamped using a 100 MHz clock and recorded by the triggerless Total Data Readout (TDR) acquisition system [18]. The data were sorted and analysed using the GRAIN [19] and ROOT [20] software packages, respectively.

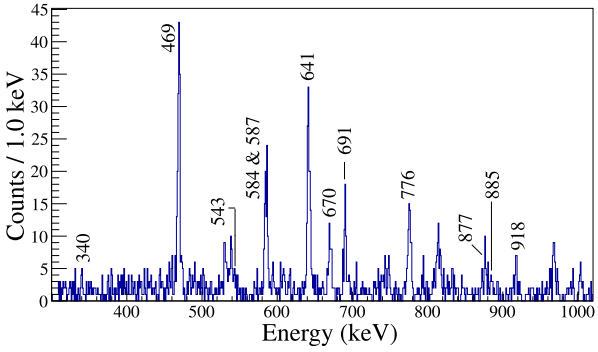

Fig. 1. In-beam Doppler-corrected γ-ray spectrum correlated with the recoil-$\alpha\alpha$ decay chain of the ^{110}Xe ions implanted at the MARA focal plane. Only γ-ray transitions placed in the level scheme are marked with their corresponding transition energies.

3. Analysis

Prompt γ-rays of ^{110}Xe were selected using the identification of the subsequent α decays of ^{110}Xe and its daughter, ^{106}Te, after the recoil implantation. The α decay of ^{110}Xe has been reported to have E_α = 3717(19) keV, $T_{1/2}$ = 93(3) ms [10], and b_α = 64(35) % [21]. The ^{106}Te is a pure α emitter, b_α = 100% with E_α = 4128(9) keV and $T_{1/2}$ = 70(17) μs [22,23]. In the analysis, the correlation times between a recoil implant and its subsequent α decays were limited to 500 ms and 350 μs, respectively. In addition, a gate on the 3720 keV and 4120 keV α-decay energies with a width of 80 keV for the first and the second decay were imposed, respectively, to identify the prompt γ rays of ^{110}Xe. In total, 2460(50) ions of ^{110}Xe were identified at the MARA focal plane and correlated with γ-rays detected by the JUROGAM 3 array. The corresponding Doppler-corrected γ-ray energy spectrum recorded at the target position is shown in Fig. 1. Because of the very stringent selection mentioned above, this spectrum is very clean, with a negligible background, and therefore all the γ rays observed can be safely assigned to ^{110}Xe. Their energies are listed in Table 1 as well as their relative intensities and the spin and parity assignments proposed for the levels involved.

The present experimental data show a significant increase of statistics in comparison with the results obtained by Sandzelius et al. [10], thus allowing for the identification of several new transitions that will be placed in the level scheme based primarily on the γ-γ coincidence data. Despite its increase, the statistics, when requiring γ-γ coincidences, prevented anyway to obtain spectra with peak areas exceeding 2-3 counts, except for the two strongest transitions at 469 and 641 keV. However, given the negligible background, even 1 or 2 counts at the expected channels can prove the coincidence relation of two lines present in the spectrum of Fig. 1. It is nevertheless important to keep in mind that for the weakest transitions, the probability of having zero coincidence events with the most intense transitions that are in coincidence can be calculated, using a binomial distribution, to be more than 40%. In order to cope with this issue, so-called sum spectra, obtained by summing spectra gated on selected transitions, were used. Indeed, the

Table 1
Observed γ-ray transitions and intensities in ^{110}Xe. Intensities are given relative to the $(2^+) \rightarrow 0^+$ transition. Their spins and parities for the initial and final states are assigned from the systematics of the even-even xenon isotopes [5–8,10]. The transitions not placed in the level scheme are also listed. The uncertainty on the energies of most transitions is around ±1 keV, except for the weakest ones where an uncertainty of ±2 keV is adopted.

E_γ [keV]	I_i^π	I_f^π	I_{rel} [%]
340(2)	(5^-)	(3^-)	7(4)
469(1)	(2^+)	0^+	100(18)
531(1)	-	-	23(10)
539(1)	-	-	23(10)
543(2)	(3^-)	(4^+)	8(6)
584(1)	(7^-)	(5^-)	30(15)
587(1)	(9^-)	(7^-)	39(15)
641(1)	(4^+)	(2^+)	86(25)
644(1)	-	-	39(15)
670(1)	(11^-)	(9^-)	28(12)
691(1)	(7^-)	(6^+)	41(15)
776(1)	(6^+)	(4^+)	57(19)*
776(1)	(10^+)	(8^+)	57(19)*
779(2)	-	-	13(8)
814(1)	-	-	35(14)
877(1)	(8^+)	(6^+)	23(12)
885(2)	(5^-)	(4^+)	11(8)
918(2)	(13^-)	(11^-)	18(10)
968(1)	-	-	40(17)
1003(2)	-	-	16(10)

* The intensity of the 776 keV transition represents the sum of intensities of two transitions.

peaks that are not random coincidences will be enhanced in the sum spectra. In a few cases, stringent energy balance considerations supported by coincidence data were also of help in building the level scheme.

Prior to the present work, three γ rays with energies of 470 keV, 643 keV and 777 keV were identified by Sandzelius et al. in ^{110}Xe and assigned as the $(2^+) \rightarrow 0^+$, $(4^+) \rightarrow (2^+)$ and $(6^+) \rightarrow (4^+)$ transitions, respectively [10]. These transitions correspond, with slight differences in energy, to the three most intense γ rays highlighted in Fig. 1 and listed in Table 1. Fig. 2 a) to c) show the recoil-α-α correlated γ-ray spectra gated on these γ-ray transitions, which appear in coincidence with all the most intense γ rays observed.

The other most intense peaks in Fig. 1 include the doublet of transitions at 584 and 587 keV and the line at 691 keV. The key transitions that allow to establish in ^{110}Xe a new structure (the octupole band) beside the ground state band are those at 584 and 691 keV. They are in fact not in coincidence with each other, but both of them are in coincidence with the $(2^+) \rightarrow 0^+$, $(4^+) \rightarrow (2^+)$ transitions, and few other transitions, such as 587 and 670 keV, lying above, see Fig. 2 e) to g). Furthermore, the 584-keV line is not in coincidence with the $(6^+) \rightarrow (4^+)$ transition whereas the 691 keV is. These data suggest that the 4^+ state at 1110 keV is populated by two different decays from a new state at 2578 keV. One is the sequence of γ rays at 691 and 776 keV while the other one is more fragmented since only one reasonably strong transition, the 584-keV γ ray, appears. This means that if we assume that the 584-keV transition depopulates the 2578-keV state, the other new level at 1994 keV decays with more than one branch. The energy difference between the 1994-keV level and the 4^+ state at 1110 keV is 884 keV, which corresponds, within the errors, to the energy of the 885-keV line observed in the γ-ray spectrum of Fig. 1. In the spectrum gated on the 885-keV line, see Fig. 2 h), the only channel with 2 counts is the one corresponding to 584 keV, thus strongly supporting, together with the energy balance considerations, the coincidence among the two transitions. Two other weak γ rays are observed in Fig. 1 as belonging to ^{110}Xe at energies of 340 and 543 keV, whose sum corresponds within errors to the energy difference of the 1994- and 1110-keV levels. We propose them as the second branch sequence, having both of them some counts in coincidence with the 584-keV transition. The intensities of the three transitions involved in the decay of the (5^-) state, see Table 1, are consistent with the level scheme.

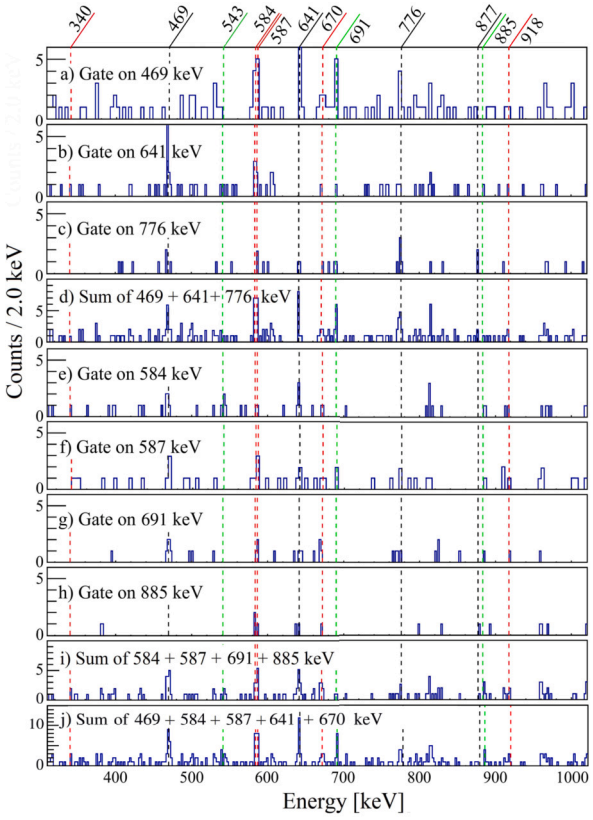

Fig. 2. Recoil-α-α tagged γ-γ coincidence spectra obtained by gating on a) 469 keV, b) 641 keV, c) 776 keV, d) the sum of the 469, 641, and 776 keV, e) 584 keV, f) 587 keV, g) 691 keV, h) 885 keV, i) the sum of 584, 587, 691, and 885 keV, and j) the sum of 469, 641, 584, 587, and 670 keV. The vertical lines correspond to the energy of the transitions placed in the level scheme of ^{110}Xe: in black for the γ rays belonging to the ground-state band, in red for the ones of the octupole band and in green for the ones connecting the two bands.

Spin and parities of the new levels are adopted in analogy with the neighbouring ^{112}Xe [5] and ^{114}Xe [6–8] nuclei. The 691-keV γ ray is thus identified as the $(7^-) \rightarrow (6^+)$ E1 transition, while the 584- and 885-keV γ rays as the $(7^-) \rightarrow (5^-)$ E2, and $(5^-) \rightarrow (4^+)$ E1, transitions. The two transitions of 340 and 543 keV are assigned to the $(5^-) \rightarrow (3^-)$ and $(3^-) \rightarrow (4^+)$ decays respectively. New γ rays at 587, 670, and 918 keV are observed in this work in coincidence with the transitions de-exciting the (7^-) level at 2578 keV, as shown in Fig. 2 e) and g). Hence, following arguments based on intensity balance and systematics of the even-even xenon isotopes, these γ-rays were assigned as the $(9^-) \rightarrow (7^-)$, $(11^-) \rightarrow (9^-)$, and $(13^-) \rightarrow (11^-)$ transitions, respectively. Having placed these new transitions above the (7^-) state, we can now add together the spectra in coincidence with the three lines at 584, 587, and 670 keV lying above the (5^-) state, and the two lines 469 and 641 keV lying below the (4^+) state, as shown in Fig. 2 j). In this spectrum, the transitions at 340, 543, and 885 keV, that define the (3^-) and (5^-) states in ^{110}Xe, appear enhanced confirming their placement in the level scheme. The γ-ray line at 776 keV cannot be resolved by another coincident line of the same energy. Furthermore, this doublet is in coincidence with another transition at 877 keV, see Fig. 2 c). By comparing these data with the energies and intensities in the ground state band of ^{112}Xe [5], we assign the 877-keV and the second 776-keV lines as the $(8^+) \rightarrow (6^+)$ and $(10^+) \rightarrow (8^+)$ transitions, respectively. Finally, two other γ rays at 814 and 968 keV belong to ^{110}Xe, as shown in Fig. 2 i) and j), and they appear to be in coincidence with transitions populating the negative parity states. Similar γ-ray transitions were also observed

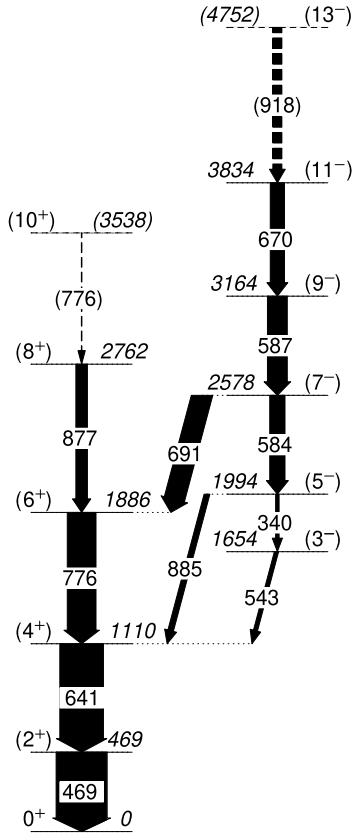

Fig. 3. Level scheme of ^{110}Xe constructed in the present work. The widths of the arrows correspond to the relative intensities of the γ-ray transitions. Dashed lines represent tentative levels and transitions.

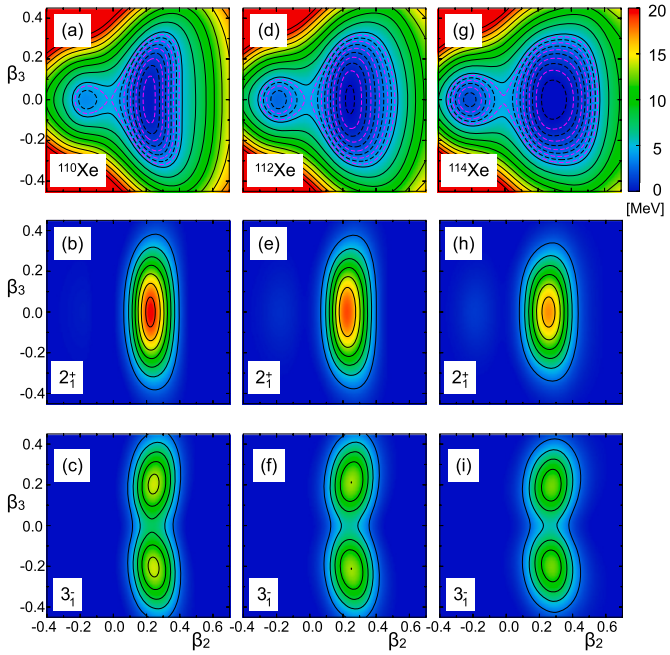

Fig. 4. (Top panel) HFB energies -normalized to the absolute minimum of each curve, see energy scale in the colorbar. (Middle panel) 2_1^+, and (bottom panel) 3_1^- collective wave functions -red (blue) means large (small) contributions to the wave function and the sum is normalized to one- as a function of (β_2, β_3) for (a)-(c) ^{110}Xe, (d)-(f) ^{112}Xe, and (g)-(i) ^{114}Xe isotopes.

in ^{112}Xe [5] and ^{114}Xe [7], but they could only be placed in the level scheme of ^{114}Xe [7]. Due to the statistics and the unknown side-band structures in the ^{112}Xe case, it was not possible to place them in this work. The deduced level scheme for ^{110}Xe is shown in Fig. 3. As previously mentioned, it is based on the γ-γ coincidences presented in Fig. 2 a) to j), the relative intensities of Table 1, and the systematics of the neighbouring even-even xenon isotopes.

4. Discussion

The excitation energy of the 2^+ and 4^+ states, which are lower than would be expected from the systematics, indicates that the ground-state deformation in ^{110}Xe is similar to its neighbouring even-even xenon isotopes. In addition, the presence of a negative-parity band connected to the ground-state band via E1 transitions shows the relevance of the octupole degree of freedom in this nucleus. Self-Consistent Mean-Field methods, like Hartree-Fock-Bogoliubov (HFB), and their Beyond-Mean-Field (BMF) extensions, are very suitable tools to study the collective dynamics of atomic nuclei in the whole nuclear chart with interactions that are not fitted to any particular region [24,25]. They are based on the variational principle and allow to find reasonable approximations to the exact many-body energies and wave functions. One of the most advanced BMF techniques is the so-called Symmetry-Conserving Configuration Mixing (SCCM) method with EDF. In the present work, the SCCM method is implemented with the well-tested Gogny D1S EDF as the underlying nucleon-nucleon interaction [25]. As we are interested in the interplay between quadrupole, and octupole degrees of freedom, a SCCM implementation that includes the mixing of parity, particle number, and angular momentum projected HFB states defined along axially symmetric quadrupole and octupole deformation parameters, (β_2, β_3), has been used [25,26]. An additional analysis of the positive parity bands has been carried out with SCCM calculations that explore both axial and triaxial quadrupole shapes. The reader is referred to Refs. [25–27] for a more detailed description of the SCCM method and the different implementations used in the present work.

In Fig. 4.(a) the Total Energy Surface (TES) obtained with the constrained HFB method is depicted along the axial (β_2, β_3) plane. A $\beta_3 = 0$, reflection-symmetric minimum is found at $\beta_2 = 0.24$. However, the minimum is very flat and large fluctuations of β_3 are expected. In panels (b) and (c) of the same figure, the collective wave functions for the 2_1^+ and 3_1^- states are shown. The 2_1^+ wave function is peaked at $\beta_2 = 0.24$ and $\beta_3 = 0$ and it is interpreted as the $J = 2$ member of the ground-state rotational band. On the other hand, the wave function of the 3_1^- state has maxima at $\beta_2 = 0.24$ and $\beta_3 = \pm 0.2$. This suggests that the corresponding state is quadrupole deformed with strong dynamic octupole correlations. Based on simple assumptions, nuclei around $N = 56$ and $Z = 56$ are expected to show strong octupole correlations. However, they are not strong enough in the Xe region to lead to permanent octupole deformation. The experimental and theoretical excitation energies of the lowest positive and negative parity rotational bands are presented in Fig. 5. The excitation energy of the 2_1^+ and 3_1^- states comes out higher in energy than the experimental data, but it is a known feature in this framework if we take into account that an "universal" interaction is being used. Unfortunately, electromagnetic transition strengths have not been measured in the present work, and therefore, there is no direct experimental data to compare with our predictions. However, the ratio of reduced transition probabilities, $B(E1)/B(E2)$, between the negative- and positive-parity band can be determined by analysing the measured intensities of the E1 and E2 transitions involved. This ratio is expected to increase with increasing octupole correlations. Despite the low-intensity values and the large error bars in some cases, it was possible to deduce this ratio for two of the most relevant cases, the deexcitation of the 5^- and 7^- states. These values are presented in Table 2, together with the previous measured values for ^{112,114}Xe. The $B(E1)/B(E2)$ ratio for the $5^- \rightarrow 4^+$ transition in ^{110}Xe and ^{112}Xe has a similar magnitude, but much higher than in ^{114}Xe. For the $7^- \rightarrow 6^+$

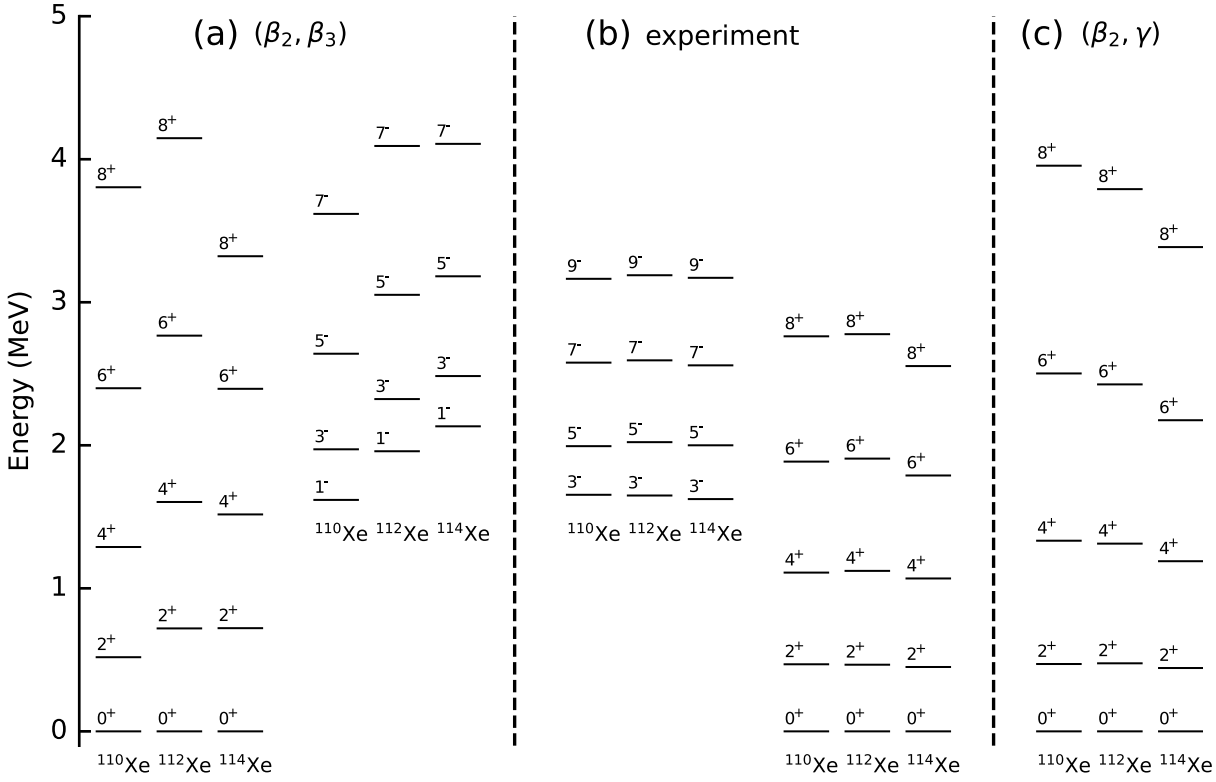

Fig. 5. Comparison between (a) axial quadrupole-octupole SCCM calculations, (b) experimental values, and (c) triaxial quadrupole SCCM calculations for ^{110,112,114}Xe isotopes.

Table 2
Experimental B(E1)/B(E2) ratios and deduced B(E1) values for the $5^- \rightarrow 4^+$ and $7^- \rightarrow 6^+$ transitions in ^{110,112,114}Xe isotopes.

	$I_i^{\pi_i} \rightarrow I_f^{\pi_f}$	$B(E1)/B(E2)$ [10^{-8} fm^{-2}]	$B(E1)$ [10^{-4} W.u.]
^{110}Xe	$5^- \rightarrow 4^+$	0.8 (7)	0.3 (3)*
	$7^- \rightarrow 6^+$	22 (13)	9.6 (59)*
^{112}Xe	$5^- \rightarrow 4^+$	2.9 (9) [5]	1.0 (3) [5]
	$7^- \rightarrow 6^+$	1.7 (8) [5]	0.6 (2) [5]
^{114}Xe	$5^- \rightarrow 4^+$	< 0.02 [7]	< 0.003 [7]
		0.046 (13) [6]	0.006 (2) [6]
	$7^- \rightarrow 6^+$	1.5 (1) [7]	0.28 (2) [7]

* Assuming a quadrupole moment of 344 efm^2, taken from the theoretical calculations.

transition, conversely, the values of this ratio are comparable for ^{112}Xe and ^{114}Xe, but significantly higher in ^{110}Xe.

Theoretical calculations can also provide insights into the nuclear structure of this nucleus. For ^{110}Xe, we have obtained a $B(E3; 3^- \rightarrow 0^+)$ value of 31 W.u. The $B(E2; 2^+ \rightarrow 0^+)$ value is 56 W.u. which corresponds to a good rotor. Concerning the $B(E1; 1^- \rightarrow 0^+)$ a value of 1.7 10^{-5} W.u. is calculated. The $B(E1)$ seems a little bit too low, but one has to keep in mind that $E1$ transition strengths are more dependent on the detailed single particle structure around the Fermi surface than on the amount of octupole correlations in the system [28,29], and therefore small $E1$ transition strengths are common in strongly correlated octupole systems. Both rotational bands are stretched compared with the experimental data, but this is a well-known deficiency of the axial model: it does not consider triaxial nor cranking wave functions (i.e., states with non-zero K values) for the intrinsic states considered in the linear combination of Eq. (4) (see Ref [30] for a discussion of this and other aspects of the present calculation). Inclusion of such cranking states will render the calculation unreasonably expensive in terms of computing power. Both in experiment and theory the two bands become alternating parity rotational bands at $J = 8^+$ indicating that octupole correlations grow stronger with angular momentum in both cases [31].

One interesting feature of the experimental levels of the ^{110,112,114}Xe isotopes is the almost constant values for the excitation energies of the 2_1^+ (469, 466 and 450 keV) and 3_1^- (1652, 1649 and 1623 keV) states (Fig. 5(b)). In the SCCM calculations, this behaviour is not fully reproduced with the exploration of axial quadrupole-octupole shapes (Fig. 5(a)). As mentioned above, the spectra of those isotopes are stretched with respect to the experimental values and the differences between the theoretical excitation energies are enhanced. Moreover, the energy of the 3_1^- states steadily increases with the number of neutrons in the present calculations. Nevertheless, the collective wave functions of the 2_1^+ and 3_1^- states are rather similar for ^{110,112,114}Xe (see Fig. 4) and we could infer that a similar collective behaviour is obtained for these isotopes. Hence, the fact that the 2_1^+ energy remains low in ^{110}Xe is related to the relatively large quadrupole deformation still present in this nucleus despite its proximity to the $N = 50$ shell closure. We have also performed SCCM calculations including quadrupole triaxial shapes [27] but without octupolarity (negative parity bands cannot be calculated) for ^{110,112,114}Xe (Fig. 5(c)). Similar conclusions can be drawn, i.e., the spectra are stretched, and the collective wave functions are similar for all the isotopes (see Fig. 6). However, in the triaxial SCCM calculations, the 2_1^+ energies are almost constant and similar to the experimental values. Additionally, we observe the relevance of the triaxial degree of freedom both in the TES (Fig. 6(a)-(c)) and in the collective wave functions (Fig. 6(d)-(f)). The most probable deformations are found at $\gamma \approx 25°$ that are consistent with the values extracted from large-scale shell-model calculations [11]. In those calculations, rather constant yrast-band energies were also predicted for ^{110,112}Xe isotopes. Moreover, they contradict a previous explanation by Sandzelius et al. [10], regarding the importance of the isoscalar neutron-proton interactions as N approaches Z.

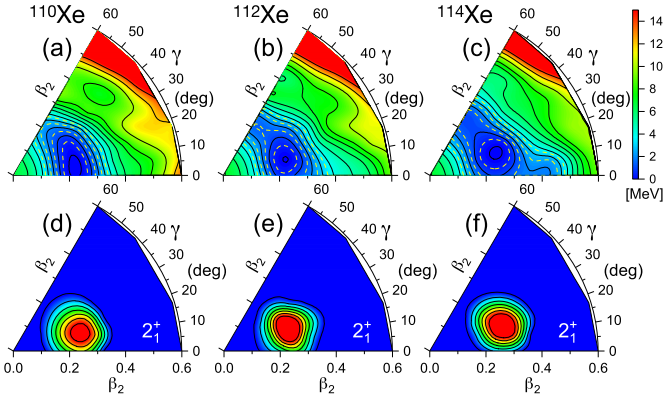

Fig. 6. (Top panel) Particle-number projected energies -normalized to the absolute minimum of each curve, see energy scale in the colorbar for (a) ^{110}Xe, (b) ^{112}Xe, and (c) ^{114}Xe isotopes. (Bottom panel) 2^+_1 collective wave functions -red (blue) means large (small) contributions to the wave function and the sum is normalized to one- as a function of (β_2, γ) for (d) ^{110}Xe, (e) ^{112}Xe, and (f) ^{114}Xe isotopes.

5. Conclusions/summary

In summary, the level scheme of ^{110}Xe has been considerably expanded in the present work, in particular, the octupole band has been identified for the first time. The spins and parities of the newly observed states have been assigned based on the systematics of the light even-even xenon isotopes. The tendency of the 2^+ and 4^+ states in ^{110,112,114}Xe indicates an abnormal increase of the ground-state deformation. Evidence for octupole correlations has been found in ^{110}Xe, such as the existence of low-lying 3^-, 5^-, and 7^- states, the inter-band E1 transitions to the 4^+, and 6^+ states in the ground-state band. Both bands exhibit alternating parity rotational states up to $J = 8^+$, and the B(E1)/B(E2) ratios increase with the J value of the initial state in the negative band. Hence, all these observations suggest an enhancement of octupole correlations as angular momentum increases. The observed transitions have been compared to the neighbouring ^{112,114}Xe and theoretical calculations using the SCCM method based on the Gogny D1S EDF. These calculations confirm that quadrupole and octupole correlations are present and the former dominate the overall collective picture of $^{110-114}$Xe isotopes. Calculations including triaxial quadrupole and octupole shapes, as well as cranking states on an equal footing, are still out of reach of the present computing capabilities. However, they would greatly help to shed light on the structure of these nuclei. In particular, the influence of triaxiality in the unexpected behaviour of the 2^+ and 3^- states. Future experiments focusing on electromagnetic transition strengths would be the ultimate benchmarks for understanding the octupole deformation in these extremely neutron-deficient xenon isotopes.

Declaration of competing interest

The authors declare that they have no known competing financial interests or personal relationships that could have appeared to influence the work reported in this paper.

Data availability

Data will be made available on request.

Acknowledgements

We want to thank the Accelerator Laboratory of the University of Jyväskylä as well as the local groups for the beam preparation and support during the beam time in the middle of a global pandemic situation. The authors would also like to thank M. Loriggiola (INFN-LNL) for manufacturing the target. This work was supported by the European Union's Horizon 2020 research and innovation programme under the Marie Skłodowska-Curie grant agreement No. 847635, by the Academy of Finland (Finland) Grant No. 307685, by the European Union's Horizon 2020 research and innovation program under grant agreement No. 771036 (ERC CoG MAIDEN), by the Spanish MICINN under PGC2018-094583-B-I00 and PID2021-127890NB-I00, by MCIN/AEI/10.13039/501100011033 Spain with grant PID2020-118265GB-C42, by Generalitat Valenciana, Spain, and EU FEDER funds, with grants PROMETEO/2019/005 and CIAPOS/2021/114. The authors acknowledge the support of GAMMAPOOL for the loan of the JUROGAM 3 detectors and the support of the GSI-Darmstadt computing facility.

References

[1] P. Butler, W. Nazarewicz, Intrinsic reflection asymmetry in atomic nuclei, Rev. Mod. Phys. 68 (1996) 349–421, https://doi.org/10.1103/RevModPhys.68.349.

[2] P. Butler, Octupole collectivity in nuclei, J. Phys. G, Nucl. Part. Phys. 43 (2016) 073002, https://doi.org/10.1088/0954-3899/43/7/073002.

[3] G. de Angelis, C. Fahlander, A. Gadea, E. Farnea, D. Bazzacco, N. Belcari, N. Blasi, P. Bizzeti, A. Bizzeti-Sona, D. de Acuña, M. De Poli, H. Grawe, A. Johnson, G. Lo Bianco, S. Lunardi, D. Napoli, J. Nyberg, P. Pavan, J. Persson, C. Rossi Alvarez, D. Rudolph, R. Schubart, P. Spolaore, R. Wyss, F. Xu, Rotation induced octupole correlations in the neutron-deficient ^{109}Te nucleus, Phys. Lett. B 437 (1998) 236–242, https://doi.org/10.1016/S0370-2693(98)00968-X.

[4] L.M. Robledo, G.F. Bertsch, Global systematics of octupole excitations in even-even nuclei, Phys. Rev. C 84 (2011) 054302, https://doi.org/10.1103/PhysRevC.84.054302.

[5] J. Smith, C. Chiara, D. Fossan, D. Lafosse, G. Lane, J. Sears, K. Starosta, M. Devlin, F. Lerma, D. Sarantites, S. Freeman, M. Leddy, J. Durell, A. Boston, E. Paul, A. Semple, I. Lee, A. Macchiavelli, P. Heenen, Excited states and deformation of ^{112}Xe, Phys. Lett. B 523 (2001) 13–21, https://doi.org/10.1016/S0370-2693(01)01339-9.

[6] S. Rugari, R. France, B. Lund, Z. Zhao, M. Gai, P. Butler, V. Holliday, A. James, G. Jones, R. Poynter, R. Tanner, K. Ying, J. Simpson, Broken reflection symmetry in ^{114}Xe, Phys. Rev. C 48 (1993) 2078, https://doi.org/10.1103/PhysRevC.48.2078.

[7] E. Paul, H. Scraggs, A. Boston, O. Dorvaux, P. Greenlees, K. Helariutta, P. Jones, R. Julin, S. Juutinen, H. Kankaanpää, H. Kettunen, M. Muikku, P. Nieminen, P. Rahkila, O. Stezowski, High-spin study of neutron-deficient ^{114}Xe, Nucl. Phys. A 673 (2000) 31–44, https://doi.org/10.1016/S0375-9474(00)00093-2.

[8] G. de Angelis, A. Gadea, E. Farnea, R. Isocrate, P. Petkov, N. Marginean, D. Napoli, A. Dewald, M. Bellato, A. Bracco, F. Camera, D. Curien, M. De Poli, E. Fioretto, A. Fitzler, S. Kasemann, N. Kintz, T. Klug, S. Lenzi, S. Lunardi, R. Menegazzo, P. Pavan, J. Pedroza, V. Pucknell, C. Ring, J. Sampson, R. Wyss, Coherent proton–neutron contribution to octupole correlations in the neutron-deficient ^{114}Xe nucleus, Phys. Lett. B 535 (2002) 93–102, https://doi.org/10.1016/S0370-2693(02)01728-8.

[9] J. Smith, C. Chiara, D. Fossan, G. Lane, J. Sears, I. Thorslund, H. Amro, C. Davids, R. Janssens, D. Seweryniak, I. Hibbert, R. Wadsworth, I. Lee, A. Macchiavelli, First observation of excited states in ^{118}Ba: possible evidence for octupole correlations in neutron-deficient barium isotopes, Phys. Rev. C 57 (1998) R1037–R1041, https://doi.org/10.1103/PhysRevC.57.R1037.

[10] M. Sandzelius, B. Hadinia, B. Cederwall, K. Andgren, E. Ganioğlu, I. Darby, M. Dimmock, S. Eeckhaudt, T. Grahn, P. Greenlees, E. Ideguchi, P. Jones, D. Joss, R. Julin, S. Juutinen, A. Khaplanov, M. Leino, L. Nelson, M. Niikura, M. Nyman, R. Page, J. Pakarinen, E. Paul, M. Petri, P. Rahkila, J. Sarén, C. Scholey, J. Sorri, J. Uusitalo, R. Wadsworth, R. Wyss, Identification of excited states in the $T_z = 1$ nucleus ^{110}Xe: evidence for enhanced collectivity near the N = Z = 50 double shell closure, Phys. Rev. Lett. 99 (2007) 022501, https://doi.org/10.1103/PhysRevLett.99.022501.

[11] E. Caurier, F. Nowacki, A. Poves, K. Sieja, Collectivity in the light xenon isotopes: a shell model study, Phys. Rev. C 82 (2010) 064304, https://doi.org/10.1103/PhysRevC.82.064304.

[12] J. Pakarinen, J. Ojala, P. Ruotsalainen, H. Tann, H. Badran, T. Calverley, J. Hilton, T. Grahn, P. Greenlees, M. Hytönen, A. Illana, A. Kauppinen, M. Luoma, P. Papadakis, J. Partanen, K. Porras, M. Puskala, P. Rahkila, K. Ranttila, J. Sarén, M. Sandzelius, S. Szwec, J. Tuunanen, J. Uusitalo, G. Zimba, The JUROGAM3 spectrometer, Eur. Phys. J. A 56 (2020) 149, https://doi.org/10.1140/epja/s10050-020-00144-6.

[13] J. Sarén, J. Uusitalo, M. Leino, P. Greenlees, U. Jakobsson, P. Jones, R. Julin, S. Juutinen, S. Ketelhut, M. Nyman, P. Peura, P. Rahkila, C. Scholey, J. Sorri, The new vacuum-mode recoil separator MARA at JYFL, Nucl. Instrum. Methods Phys. Res., Sect. B, Beam Interact. Mater. Atoms 266 (2008) 4196–4200, https://doi.org/10.1016/j.nimb.2008.05.027, https://linkinghub.elsevier.com/retrieve/pii/S0168583X08007040.

[14] J. Uusitalo, J. Sarén, J. Partanen, J. Hilton, Mass analyzing recoil apparatus, MARA, Acta Phys. Pol. B 50 (2019) 319–327, https://doi.org/10.5506/APhysPolB.50.319.

[15] E. Paul, P. Woods, T. Davinson, R. Page, P. Sellin, C. Beausang, R. Clark, R. Cunningham, S. Forbes, D. Fossan, A. Gizon, J. Gizon, K. Hauschild, I. Hibbert, A. James,

D. LaFosse, I. Lazarus, H. Schnare, J. Simpson, R. Wadsworth, M. Waring, In-beam γ-ray spectroscopy above ^{100}Sn using the new technique of recoil decay tagging, Phys. Rev. C 51 (1995) 78–87, https://doi.org/10.1103/PhysRevC.51.78.

[16] R.-D. Herzberg, Spectroscopy of superheavy elements, J. Phys. G, Nucl. Part. Phys. 30 (2004) R123–R141, https://doi.org/10.1088/0954-3899/30/4/r01.

[17] R.-D. Herzberg, P. Greenlees, In-beam and decay spectroscopy of transfermium nuclei, Prog. Part. Nucl. Phys. 61 (2008) 674–720, https://doi.org/10.1016/j.ppnp.2008.05.003.

[18] I. Lazarus, D. Appelbe, P. Butler, P. Coleman-Smith, J. Cresswell, S. Freeman, R. Herzberg, I. Hibbert, D. Joss, S. Letts, V. Pucknell, P. Regan, J. Sampson, J. Simpson, J. Thornhill, R. Wadsworth, The great triggerless total data readout method, IEEE Trans. Nucl. Sci. 48 (2001) 567–569, https://doi.org/10.1109/23.940120.

[19] P. Rahkila, Grain—a Java data analysis system for total data readout, Nucl. Instrum. Methods Phys. Res., Sect. A, Accel. Spectrom. Detect. Assoc. Equip. 595 (2008) 637–642, https://doi.org/10.1016/j.nima.2008.08.039.

[20] R. Brun, F. Rademakers, ROOT — an object oriented data analysis framework, Nucl. Instrum. Methods Phys. Res., Sect. A, Accel. Spectrom. Detect. Assoc. Equip. 389 (1997) 81–86, https://doi.org/10.1016/S0168-9002(97)00048-X.

[21] C. Mazzocchi, Z. Janas, L. Batist, V. Belleguic, J. Döring, M. Gierlik, M. Kapica, R. Kirchner, G. Lalazissis, H. Mahmud, E. Roeckl, P. Ring, K. Schmidt, P. Woods, J. Żylicz, Alpha decay of ^{114}Ba, Phys. Lett. B 532 (2002) 29–36, https://doi.org/10.1016/S0370-2693(02)01543-5.

[22] R. Page, P. Woods, R. Cunningham, T. Davinson, N. Davis, A. James, K. Livingston, P. Sellin, A. Shotter, Decays of odd-odd N - Z = 2 nuclei above ^{100}Sn: the observation of proton radioactivity from ^{112}Cs, Phys. Rev. Lett. 72 (1994) 1798–1801, https://doi.org/10.1103/PhysRevLett.72.1798.

[23] B. Hadinia, B. Cederwall, J. Blomqvist, E. Ganioğlu, P. Greenlees, K. Andgren, I. Darby, S. Eeckhaudt, E. Ideguchi, P. Jones, D. Joss, R. Julin, S. Juutinen, S. Ketelhut, K. Lagergren, A. Leppänen, M. Leino, M. Nyman, J. Pakarinen, E. Paul, M. Petri, P. Rahkila, M. Sandzelius, J. Sarén, C. Scholey, J. Uusitalo, R. Wadsworth, R. Wyss, First identification of excited states in ^{106}Te and evidence for isoscalar-enhanced vibrational collectivity, Phys. Rev. C 72 (2005) 041303R, https://doi.org/10.1103/PhysRevC.72.041303.

[24] M. Bender, P.-H. Heenen, P.-G. Reinhard, Self-consistent mean-field models for nuclear structure, Rev. Mod. Phys. 75 (2003) 121, https://doi.org/10.1103/RevModPhys.75.121.

[25] L.M. Robledo, T.R. Rodríguez, R.R. Rodríguez-Guzmán, Mean field and beyond description of nuclear structure with the Gogny force: a review, J. Phys. G, Nucl. Part. Phys. 46 (2019) 013001, http://stacks.iop.org/0954-3899/46/i=1/a=013001.

[26] R.N. Bernard, L.M. Robledo, T.R. Rodríguez, Octupole correlations in the ^{144}Ba nucleus described with symmetry-conserving configuration-mixing calculations, Phys. Rev. C 93 (2016) 061302, https://doi.org/10.1103/PhysRevC.93.061302.

[27] T.R. Rodríguez, J.L. Egido, Triaxial angular momentum projection and configuration mixing calculations with the Gogny force, Phys. Rev. C 81 (2010) 064323, https://doi.org/10.1103/PhysRevC.81.064323.

[28] B. Bucher, S. Zhu, C.Y. Wu, R.V.F. Janssens, R.N. Bernard, L.M. Robledo, T.R. Rodríguez, D. Cline, A.B. Hayes, A.D. Ayangeakaa, M.Q. Buckner, C.M. Campbell, M.P. Carpenter, J.A. Clark, H.L. Crawford, H.M. David, C. Dickerson, J. Harker, C.R. Hoffman, B.P. Kay, F.G. Kondev, T. Lauritsen, A.O. Macchiavelli, R.C. Pardo, G. Savard, D. Seweryniak, R. Vondrasek, Direct evidence for octupole deformation in ^{146}Ba and the origin of large $e1$ moment variations in reflection-asymmetric nuclei, Phys. Rev. Lett. 118 (2017) 152504, https://doi.org/10.1103/PhysRevLett.118.152504.

[29] J. Egido, L. Robledo, A systematic study of the octupole correlations in the lanthanides with realistic forces, Nucl. Phys. A 545 (1992) 589–607, https://doi.org/10.1016/0375-9474(92)90294-T.

[30] Tomás R. Rodríguez, Precise description of nuclear spectra with Gogny energy density functional methods, Eur. Phys. J. A 52 (2016) 190, https://doi.org/10.1140/epja/i2016-16190-2.

[31] E. Garrote, J.L. Egido, L.M. Robledo, Fingerprints of reflection asymmetry at high angular momentum in atomic nuclei, Phys. Rev. Lett. 80 (1998) 4398–4401, https://doi.org/10.1103/PhysRevLett.80.4398.